Ultrafast and Energy-Efficient Quenching of Spin Order: Antiferromagnetism Beats Ferromagnetism

Nele Thielemann-Kühn,[1,2,*] Daniel Schick,[1] Niko Pontius,[1] Christoph Trabant,[1,2,3] Rolf Mitzner,[1] Karsten Holldack,[1] Hartmut Zabel,[4] Alexander Föhlisch,[1,2] and Christian Schüßler-Langeheine[1]

[1]*Institut für Methoden und Instrumentierung der Forschung mit Synchrotronstrahlung, Helmholtz-Zentrum Berlin für Materialien und Energie GmbH, Albert-Einstein-Straße 15, 12489 Berlin, Germany*

[2]*Institut für Physik und Astronomie, Universität Potsdam, Karl-Liebknecht-Straße 24/25, 14476 Potsdam, Germany*

[3]*II. Physikalisches Institut, Universität zu Köln, Zülpicher Straße 77, 50937 Köln, Germany*

[4]*Institut für Physik, Johannes-Gutenberg-Universität Mainz, Staudingerweg 7, 55128 Mainz, Germany*

(Received 15 March 2017; revised manuscript received 20 September 2017; published 6 November 2017)

By comparing femtosecond laser pulse induced ferro- and antiferromagnetic dynamics in one and the same material—metallic dysprosium—we show both to behave fundamentally different. Antiferromagnetic order is considerably faster and much more efficiently reduced by optical excitation than its ferromagnetic counterpart. We assign the fast and extremely efficient process in the antiferromagnet to an interatomic transfer of angular momentum within the spin system. Our findings imply that this angular momentum transfer channel is effective in other magnetic metals with nonparallel spin alignment. They also point out a possible route towards energy-efficient spin manipulation for magnetic devices.

DOI: 10.1103/PhysRevLett.119.197202

Striving for novel concepts for faster and more energy-efficient data processing and storage, a wealth of experimental and theoretical studies in the field of ultrafast magnetic dynamics has been carried out [1–14]. This entailed the understanding that a speed limit for spin manipulation is governed by the achievable angular momentum transfer. For any change of magnetic order fundamental conservation laws require transfer of angular momentum associated with the atomic magnetic moments [1,15]. This is particularly relevant when magnetic order is to be affected on ultrashort time scales, e.g., by femtosecond laser-pulse excitation. Here the angular momentum transfer effectively limits the speed of magnetic dynamics. Various transfer channels have been identified including local scattering processes [2–5] as well as spin transport [6–9], and their relative importance for ultrafast magnetic dynamics is the subject of intense debate [1,3,10–12]. Changing ferromagnetic (FM) order via local processes requires angular momentum transfer out of the spin system into an external reservoir like the lattice. In contrast, the change of antiferromagnetic (AFM) order with vanishing net magnetization, could be achieved by redistribution of angular momentum within the spin system itself; transfer of angular momentum into other degrees of freedom is not required. One would therefore expect any change of AFM order to occur faster than modifications of FM order.

So far, AFM dynamics has been mostly studied experimentally in transition-metal oxides and has been found to proceed over a wide range of time scales including ultrafast dynamics within 230 fs [16], but also much slower dynamics on picosecond time scales [17]. In ferrimagnetic metallic alloys of $3d$ and $4f$ metals, ultrafast angular momentum transfer between antiferromagnetically exchange-coupled sublattices was observed [13,18]. These results, however, are not straightforwardly comparable to the wealth of work about FM metals: for $3d$-$4f$ alloy dynamics, static inhomogeneity has been shown to play a crucial role [19]; and in oxides the exchange coupling mechanisms are different to those in metals. This renders quantitative comparison with the thoroughly studied elemental ferromagnets ambiguous. Already within one material class any magnetic dynamics—FM as well as AFM—is expected to depend on the size of the magnetic moment [20] and on material properties like the spin-orbit, spin-lattice, and electron-lattice interaction [1]. To avoid such complications, we compare FM and AFM dynamics in the most direct way in one and the same material: metallic dysprosium (Dy).

Dy is FM at low temperatures and has a helical AFM phase between 85 K and 178 K [21], see Fig. 1. The strongly localized $4f$ magnetic moments ($10\mu_B$ per atom) are magnetically coupled by indirect (RKKY) exchange through intra-atomic spin polarization of mostly $5d$ states in the ($5d6s$) conduction band [22,23]. AFM and paramagnetic Dy has hcp symmetry; the FM phase shows an orthorhombic distortion [24]. In the FM phase all $4f$ spins are parallel aligned within the basal ab planes, see Fig. 1(a). In the AFM phase, the $4f$ spins within each ab plane remain ferromagnetically aligned but form a helical structure along the crystallographic c axis, see Fig. 1(e).

FM and AFM $4f$ order can straightforwardly be probed with soft x rays tuned to the $3d \rightarrow 4f$ electronic excitation (M_5 edge at around 1292 eV photon energy). For FM order we used magnetic circular dichroism (MCD) in reflection

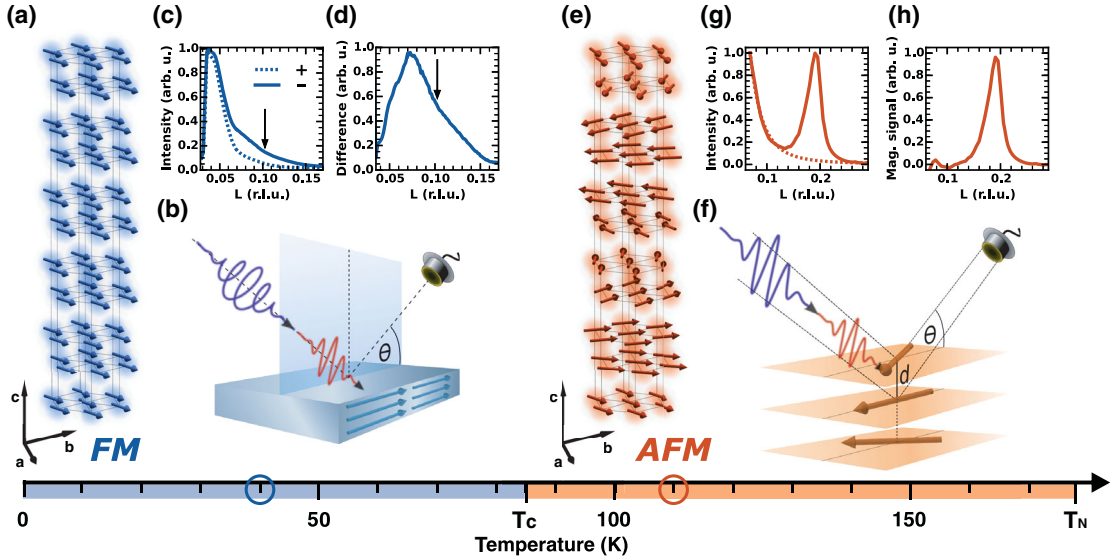

FIG. 1. (a) FM structure of the $4f$ spins. (b) Geometry for probing ferromagnetism with circularly polarized soft x rays tuned to the Dy M_5 resonance; a near-infrared laser pulse is shown as a red wave packet. (c) Specular reflectivity vs momentum transfer L, for opposite photon-helicity projections on the sample magnetization (solid and dashed lines). The difference (d) is the FM contrast and the temporal response is probed at the momentum transfer value marked by the arrow. (e) AFM spin structure. (f) Geometry for probing AFM order with linearly polarized soft x rays. (g) Magnetic Bragg peak due to the magnetic helix period length (about 5 times the crystalline unit cell or 10 atomic layers) located on a weak reflectivity background (dashed line) that has been subtracted in (h).

geometry [25,26], i.e., the effect that a FM sample reflects elliptically polarized x rays differently depending on the photon helicity projection onto the sample magnetization. For probing FM dynamics, the sample was held at 40 K. The specular reflected intensity at the maximum of the Dy M_5 absorption edge was recorded for the opposite sign of a magnetic field of 80 mT oriented in the scattering plane and parallel to the sample surface. Incidence and detection angles were set to 5° with respect to the sample surface. In order to determine the FM order parameter, the difference in reflected intensities for opposite direction of the magnetic field was taken [25].

AFM order was studied by resonant magnetic x-ray diffraction: The helical magnetic order leads to a superstructure Bragg peak [27] at $(0\,0\,\tau)$ with $\tau \approx 0.19$ in reciprocal lattice units (r.l.u.). Data in the AFM phase were recorded using linearly polarized x rays with the sample held at 110 K. The magnetic diffraction peak at $(0\,0\,\tau)$ occurs in specular geometry with an incidence angle of about 9.5° with respect to the sample surface. In order to determine the AFM order parameter the square root of the scattering signal was calculated [28].

Since resonant magnetic x-ray diffraction and magnetic circular dichroism are based on exactly the same contrast mechanism [29], a combination of both techniques allows for determining the FM and AFM order parameters in a directly comparable way. For an overview of experimental geometries and data acquisition see Fig. 1. As a sample, we chose a 120 nm thin metallic Dy film grown by molecular beam epitaxy with (0 0 1) surface orientation. The film was sandwiched between Yttrium (Y) layers to minimize strain; Niobium (Nb) served as the buffer layer and oxidation protection; sapphire was the substrate [30]. The stacking in the film was Nb(2.5 nm)/Y(3 nm)/Dy(120 nm)/Y(70 nm)/Nb(50 nm)/a-plane sapphire.

All experiments were carried out at the FemtoSpeX slicing facility at the electron storage ring BESSY II of the Helmholtz-Zentrum Berlin [31]. Magnetic dynamics was induced by 800-nm–near-infrared-laser pulses of 50 fs duration. The magnetic signal was probed with 100-fs–x-ray pulses, hitting the sample with a 6 kHz repetition rate, while the pump laser was operated at 3 kHz such that alternating signals with and without pump-laser excitation were detected. The latter were used for normalization. The overall temporal resolution was about 120 fs. For our geometry, the penetration depth for pump photons is about 21 nm [32]; the x-ray probing depth is 7 nm (12 nm) for the FM (AFM) case (see Supplemental Material [33]). The probed volume in our experiment was thus fully excited by the laser. Detailed information on the experimental setup, data acquisition, data analysis, as well as the complete set of evaluated data can be found in the Supplemental Material [33].

Typical dynamical data are presented in Fig. 2(a). The two transients demonstrate the clearly different response of the two order parameters. After an equally strong laser excitation (absorbed fluence), both magnetic order parameters are reduced, but the quenching of the AFM order is considerably and consistently stronger for all delays. Moreover, the

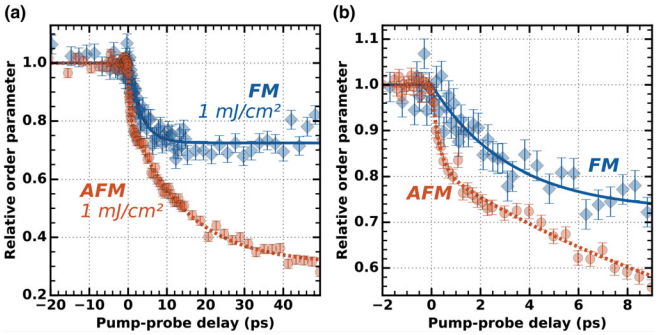

FIG. 2. (a) Pump-probe delay scans in the FM (blue) and AFM (orange) phase for an absorbed laser fluence of 1 $\mathrm{mJ/cm^2}$. The symbols denote the normalized magnetic order parameter; the lines denote exponential fits to the data. (b) First 9 ps of the delay traces on an enlarged scale.

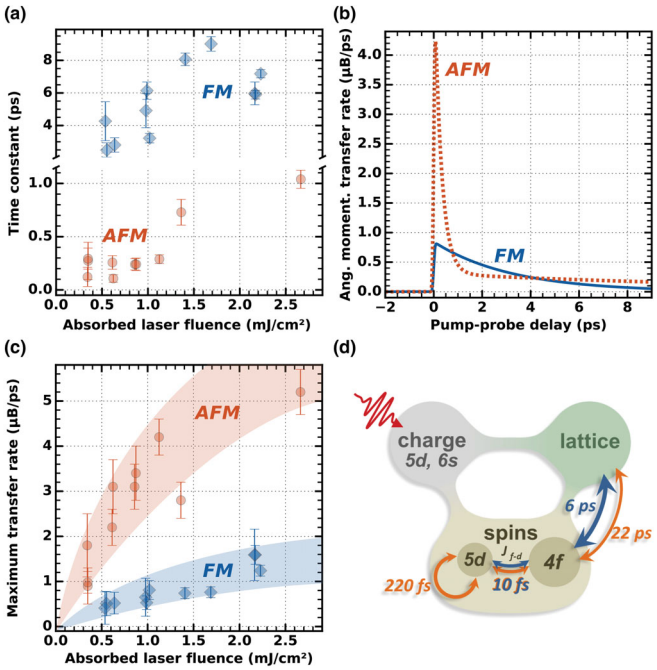

FIG. 3. (a) Short time constants for the AFM and single time constants for the FM dynamics, determined from the delay traces for different absorbed laser fluences (note broken y axis). (b) The momentary rate of average atomic angular momentum transfer derived from the exponential fits in Fig. 2(a). (c) Maximum momentary angular momentum transfer rate deduced from the delay traces for different absorbed laser fluences. The shaded areas are guides to the eye. (d) Channels of angular momentum transfer active in the AFM (orange arrows) and FM (blue arrows) phase of Dy (see text).

shapes of the two transients are significantly different. Zooming into the first 9 ps [Fig. 2(b)] reveals the initial AFM order parameter loss to occur much faster than its FM counterpart. For AFM dynamics in Fig. 2 we find an initial fast reduction with an exponential time constant of (290 ± 40) fs followed by a slower one of (14 ± 1) ps. In contrast, the FM dynamics occurs with a single time constant of (3.2 ± 0.3) ps. The lines in Figs. 2(a) and 2(b) show results of least square fits to double or single exponential decay models (see Supplemental Material [33]).

A fluence dependent investigation, see Fig. 3(a), shows the initial AFM decay time constant to vary very little for low absorbed fluences up to 1.2 $\mathrm{mJ/cm^2}$ with an average value of (220 ± 70) fs. For higher fluences, the decay becomes slower, reading 1040 fs for the highest fluence considered in this work. Remarkably, all initial AFM dynamics are significantly faster than the single time constants in the FM phase; the latter ones on average amount to (6 ± 2) ps [Fig. 3(a)]. The difference between FM and AFM dynamics becomes even more pronounced comparing the momentary rate of atomic angular momentum transfer [Fig. 3(b)]. We define the (momentary) angular momentum transfer rate as the change of the magnetic order parameter per time. The maximum transfer rate in the AFM phase is more than 5 times higher than in the FM phase. This trend is true for a wide range of laser-excitation fluences. In Fig. 3(c) we present the maximum measured angular momentum transfer rate vs the absorbed laser fluence. The maximum AFM transfer rates are always higher by a factor of 4 to 5. Ultrafast reduction of spin order in the antiferromagnet is hence more energy efficient than in the ferromagnet.

We note that in between the base temperatures of the experiments (40 K and 110 K, respectively) the static order parameter changes by less than 15%. This small change can not cause such different magnetic dynamics. The higher energy efficiency along with the faster spin dynamics for the AFM phase is a true consequence of the different spin structures.

In principle, the energy deposited by the laser above a fluence of about 1 $\mathrm{mJ/cm^2}$ for the FM and about 1.8 $\mathrm{mJ/cm^2}$ for the AFM case [38] would be sufficient to heat the sample across the nearest phase transition. We find, however, no indications for such an effect within the time window of our experiment. The clearest indication for the absence of an equilibrium phase transition is the residual FM and AFM order parameter we find even after a 50 ps delay and for fairly high fluences (see Supplemental Material [33]); an equilibrium phase transition would lead to a complete loss of the respective order parameter. In fact, a long lasting nonequilibrium between the Dy spin system and lattice after photoexcitation was also observed in a recent structural dynamics study [39].

In the following we discuss the angular momentum transfer channels responsible for the observed behavior. We assign the difference between FM and AFM dynamics for short delay times to an angular momentum transfer channel only effective in magnetic systems like antiferromagnets, i.e., where spin orientations are not parallel.

This transfer channel is essentially based on interatomic spin hopping.

Since a direct excitation of $4f$ electrons (3.8 eV binding energy) or a transition of $5d6s$ electrons into unoccupied $4f$ states (2 eV above Fermi level) is not possible in both magnetic phases with the pump photon-energy of 1.5 eV [40], the pump-laser pulse essentially excites delocalized $5d6s$ electrons. In the AFM phase these excited electrons with their spins initially aligned parallel to the local $4f$ spins hop to adjacent sites with nonparallel $4f$ spins. This brings about a disordering of the $5d$-spin subsystem. Subsequently this disorder is imposed onto the $4f$ subsystem via the strong $4f$-$5d$ coupling [14]. Note that such interatomic spin transfer also occurs in the FM phase but—owing to the allover parallel spin alignment–will not cause any demagnetization and has therefore not been observed in FM dynamics studies.

For discussing the FM case it is instructive to compare Dy with the neighboring lanthanide ferromagnet terbium (Tb), which has a very similar electronic structure. For Tb, two different channels transferring angular momentum from $4f$ electrons to the lattice have been identified: (i) via fast intra-atomic exchange with the delocalized $5d$ valence electrons in the presence of hot electrons and (ii) the slower direct $4f$-spin-lattice coupling [14]. Interestingly, the fast decay channel (i) is not found in our Dy FM data. Since structural and magnetic properties of Dy and Tb are very similar, major differences in $4f$-$5d$ or $4f$-lattice coupling are not to be expected. A main difference between the Tb experiment in Ref. [14] and our Dy experiment is the sample thickness, though: the Tb film in Ref. [14] was 10 nm thick; while our Dy sample had a thickness of 120 nm [41]. It is to be expected that variation of the film thickness in this range (10 nm are 35 monolayers) neither affects the $4f$-$5d$ nor the $4f$-lattice coupling. On the other hand, spin transport should strongly depend on the sample dimensions as it involves spin currents into nonmagnetic regions [6]. For our thick Dy film only the very thin nonmagnetic cap layer is near the probed volume while the thick nonmagnetic Y buffer layer is far away from the photoexcited regions. We therefore speculate that the fast time constant seen before in Tb may actually not be due to channel (i) but rather be caused by spin transport.

We would like to stress that the question about the existence of channel (i) in FM Dy does not affect our conclusion about the interatomic spin transfer being fast and energy efficient: even if we missed a fast FM transfer channel in our Dy sample, this channel can be expected to have a similar time constant as the one in Tb. For the latter one, (740 ± 250) fs was found [14,42], which is still much slower than our result for the fast AFM dynamics in Dy. We note that in a recent magneto-optical Kerr effect (MOKE) study of Dy a fast 300-fs dynamics for the out-of-plane magnetization has been observed [43]. Similar time scales were also detected in MOKE experiments from FM Gd [44] and were assigned to nonmagnetic laser-induced changes of the optical sample properties [45,46] nonrepresentative of the $4f$-magnetic dynamics.

Coming back to the second, slower AFM dynamics with a time constant of (22 ± 7) ps: this and the FM time constant of (6 ± 2) ps are of similar order of magnitude as the time constant in Tb (8 ps) related to the $4f$-spin-lattice coupling [channel (ii)] and should have the same origin. The quantitative difference we find between the two Dy phases hint to stronger $4f$-lattice coupling in the FM phase [47], which agrees with the observation that in FM Dy the $4f$ spins are confined by a uniaxial in-plane anisotropy which is absent in the AFM phase [22]. We found no indications for an even slower AFM time scale of 200 ps as reported by Langner *et al.* who studied the magnetic diffraction signal in Dy albeit with a much lower temporal resolution of 70 ps [43].

In Fig. 3(d) we present an overview of the different angular momentum transfer channels with their characteristic time scales, including the interatomic spin transfer channel. In AFM Dy the interatomic transfer channel via hopping of $5d$ electrons to adjacent atomic sites is effective in addition to those channels available in the FM phase. The opening of this channel leads to an up to 30 times faster reduction of the magnetic order compared to the FM phase. For the $4f$-$5d$ coupling we refer to the value of 10 fs following Ref. [23,48].

Our case study on Dy shows that for one and the same material the reduction of spin order is much faster and more energy-efficiently achieved when spins are antiferromagnetically aligned compared to FM spin order. Generally, any nonparallel spin alignment would allow us to change the order parameter by redistributing angular momentum within the spin system. Since in the helical phase of Dy the angle between neighboring spins is only of the order of 34°, even stronger effects may occur for larger relative angles. Our results apply primarily to $4f$ metals; since the angular momentum redistribution occurs through scattering of $5d$ electrons, similar effects can be expected as well in other systems where magnetic dynamics is dominated by d-electron scattering.

The highly efficient ultrafast interatomic transfer of angular momentum between nonparallel spins may define a route towards more energy-efficient ultrafast spin manipulation in devices. Nonparallel coupled magnetic moments may serve as spin sinks that reduce the energy required to manipulate spin order or allow for tuning time constants. The all-optical switching in, e.g., GdFeCo occurs via an almost complete quenching of the magnetization in the material [18]. Most of the angular momentum needs to be transferred out of the $4f$ system before switching sets in. Based on our finding, the energy needed to reach this transfer should be much lower when nonparallel $4f$ spins are available either within the same

material or possibly even in a multilayer structure. Clever material design can make use of this effect to reduce the energy needed for ultrafast spin manipulation like optically induced magnetic switching.

Work was supported by the BMBF (Contract No. 05K10PK2). D. S. acknowledges the Helmholtz Association for funding via the Helmholtz Postdoc Program No. PD-142. N. T.-K. acknowledges the Helmholtz Association for funding via the Helmholtz Virtual Institute "Dynamic Pathways in Multidimensional Landscapes."

N. T.-K., D. S., N. P., C. T., H. Z., and C. S.-L. planned and carried out the experiment with experimental support from R. M. and K. H.; H. Z. prepared the sample; N. T.-K., D. S., and N. P. analyzed the data; N. T.-K., N. P., D. S., and C. S.-L. wrote the Letter with help from the other authors.

*Present address: Fachbereich Physik, Freie Universität Berlin, Arnimallee 14, 14195 Berlin, Germany.
nele.thielemann@helmholtz-berlin.de

[1] A. Kirilyuk, A. V. Kimel, and T. Rasing, Rev. Mod. Phys. **82**, 2731 (2010).
[2] D. Steiauf and M. Fähnle, Phys. Rev. B **79**, 140401 (2009).
[3] B. Koopmans, G. Malinowski, F. Dalla Longa, D. Steiauf, M. Fähnle, T. Roth, M. Cinchetti, and M. Aeschlimann, Nat. Mater. **9**, 259 (2010).
[4] A. J. Schellekens and B. Koopmans, Phys. Rev. Lett. **110**, 217204 (2013).
[5] B. Y. Mueller, T. Roth, M. Cinchetti, M. Aeschlimann, and B. Rethfeld, New J. Phys. **13**, 123010 (2011).
[6] M. Battiato, K. Carva, and P. M. Oppeneer, Phys. Rev. Lett. **105**, 027203 (2010).
[7] G. Malinowski, F. Dalla Longa, J. H. H. Rietjens, P. V. Paluskar, R. Huijink, H. J. M. Swagten, and B. Koopmans, Nat. Phys. **4**, 855 (2008).
[8] D. Rudolf *et al.*, Nat. Commun. **3**, 1037 (2012).
[9] A. Eschenlohr, M. Battiato, P. Maldonado, N. Pontius, T. Kachel, K. Holldack, R. Mitzner, A. Föhlisch, P. M. Oppeneer, and C. Stamm, Nat. Mater. **12**, 332 (2013).
[10] S. Essert and H. C. Schneider, Phys. Rev. B **84**, 224405 (2011).
[11] T. Roth, A. J. Schellekens, S. Alebrand, O. Schmitt, D. Steil, B. Koopmans, M. Cinchetti, and M. Aeschlimann, Phys. Rev. X **2**, 021006 (2012).
[12] T. Ostler *et al.*, Nat. Commun. **3**, 666 (2012);
[13] N. Bergeard, V. López-Flores, V. Halté, M. Hehn, C. Stamm, N. Pontius, E. Beaurepaire, and C. Boeglin, Nat. Commun. **5**, 3466 (2014).
[14] M. Wietstruk, A. Melnikov, C. Stamm, T. Kachel, N. Pontius, M. Sultan, C. Gahl, M. Weinelt, H. A. Dürr, and U. Bovensiepen, Phys. Rev. Lett. **106**, 127401 (2011).
[15] A. Einstein and W. de Haas, Verh. Dtsch. Phys. Ges. **17**, 152 (1915).
[16] M. Fiebig, N. P. Duong, T. Satoh, B. B. Van Aken, K. Miyano, Y. Tomioka, and Y. Tokura, J. Phys. D **41**, 164005 (2008).
[17] R. I. Tobey *et al.*, Phys. Rev. B **86**, 064425 (2012).
[18] I. Radu *et al.*, Nature (London) **472**, 205 (2011).
[19] C. E. Graves *et al.*, Nat. Mater. **12**, 293 (2013).
[20] I. Radu *et al.*, SPIN **05**, 1550004 (2015).
[21] D. R. Behrendt, S. Legvold, and F. H. Spedding, Phys. Rev. **109**, 1544 (1958).
[22] J. Jensen and A. R. Mackintosh, *Rare Earth Magnetism: Structures and Excitations*, International Series of Monographs on Physics (Clarendon Press, Oxford, 1991), ISBN 9780198520276.
[23] R. Ahuja, S. Auluck, B. Johansson, and M. S. S. Brooks, Phys. Rev. B **50**, 5147 (1994).
[24] F. J. Darnell, Phys. Rev. **130**, 1825 (1963).
[25] H.-C. Mertins, D. Abramsohn, A. Gaupp, F. Schäfers, W. Gudat, O. Zaharko, H. Grimmer, and P. M. Oppeneer, Phys. Rev. B **66**, 184404 (2002).
[26] S. Macke and E. Goering, J. Phys. Condens. Matter **26**, 363201 (2014).
[27] H. Ott, C. Schüßler-Langeheine, E. Schierle, E. Weschke, and G. Kaindl, Phys. Rev. B **82**, 214408 (2010).
[28] H. Ott, C. Schüßler-Langeheine, E. Schierle, A. Y. Grigoriev, V. Leiner, H. Zabel, G. Kaindl, and E. Weschke, Phys. Rev. B **74**, 094412 (2006).
[29] S. W. Lovesey and S. P. Collins, *X-Ray Scattering and Absorption by Magnetic Materials* (Oxford University Press, Oxford, 1996), ISBN 9780198517375.
[30] V. Leiner, M. Ay, and H. Zabel, Phys. Rev. B **70**, 104429 (2004).
[31] K. Holldack *et al.*, J. Synchrotron Radiat. **21**, 1090 (2014).
[32] S. Adachi, *The Handbook on Optical Constants of Metals* (World Scientific Publishing Co. Pte. Ltd., Singapore, 2012), ISBN 978-981-4405-95-9.
[33] See Supplemental Material at http://link.aps.org/supplemental/10.1103/PhysRevLett.119.197202 for detailed information on methods and data analysis, which includes Refs. [34–37].
[34] D. Schick, L. Le Guyader, N. Pontius, I. Radu, T. Kachel, R. Mitzner, T. Zeschke, C. Schüßler-Langeheine, A. Föhlisch, and K. Holldack, J. Synchrotron Radiat. **23**, 700 (2016).
[35] M. Newville, T. Stensitzki, D. Allen, and A. Ingargiola, *LMFIT: Non-Linear Least-Square Minimization and Curve-Fitting for Python* (Zenodo, Geneva, Switzerland, 2014).
[36] M. K. Wilkinson, W. C. Koehler, E. O. Wollan, and J. W. Cable, J. Appl. Phys. **32**, S48 (1961).
[37] J. D. Hunter, Comput. Sci. Eng. **9**, 90 (2007).
[38] M. Griffel, R. E. Skochdopole, and F. H. Spedding, J. Chem. Phys. **25**, 75 (1956).
[39] A. von Reppert, J. Pudell, A. Koc, M. Reinhardt, W. Leitenberger, K. Dumesnil, F. Zamponi, and M. Bargheer, Struct. Dyn. **3**, 054302 (2016).
[40] S. Lebègue, A. Svane, M. I. Katsnelson, A. I. Lichtenstein, and O. Eriksson, J. Phys. Condens. Matter **18**, 6329 (2006).
[41] Thin Dy films do not develop a FM phase when epitaxially grown between Y layers.
[42] A. Eschenlohr, M. Sultan, A. Melnikov, N. Bergeard, J. Wieczorek, T. Kachel, C. Stamm, and U. Bovensiepen, Phys. Rev. B **89**, 214423 (2014).
[43] M. C. Langner, S. Roy, A. F. Kemper, Y. D. Chuang, S. K. Mishra, R. B. Versteeg, Y. Zhu, M. P. Hertlein, T. E. Glover,

K. Dumesil, and R. W. Schoenlein, Phys. Rev. B **92**, 184423 (2015).
[44] M. Sultan, U. Atxitia, A. Melnikov, O. Chubykalo-Fesenko, and U. Bovensiepen, Phys. Rev. B **85**, 184407 (2012).
[45] B. Koopmans, M. van Kampen, J. T. Kohlhepp, and W. J. M. de Jonge, Phys. Rev. Lett. **85**, 844 (2000).
[46] P. M. Oppeneer and A. Liebsch, J. Phys. Condens. Matter **16**, 5519 (2004).
[47] W. Hübner and K. H. Bennemann, Phys. Rev. B **53**, 3422 (1996).
[48] This value has recently been questioned when photoemission experiments and theory results found a slower $4f-5d$ coupling for gadolinium (Gd) [49]. The authors of that study stress, however, that their results strongly depend on the low $4f$-$5d$ overlap, which is a particular property of the Gd band structure. For Dy this overlap is larger. Furthermore, a recent magnetic diffraction study on $4f$ and $5d$ dynamics in AFM holmium (similar $4f$-$5d$ overlap as in Dy), also found a very efficient $4f$-$5d$ coupling [50]. And even for Gd, theoretical predictions are diverse [51].
[49] B. Frietsch, J. Bowlan, R. Carley, M. Teichmann, S. Wienholdt, D. Hinzke, U. Nowak, K. Carva, P. M. Oppeneer, and M. Weinelt, Nat. Commun. **6**, 8262 (2015).
[50] L. Rettig *et al.*, Phys. Rev. Lett. **116**, 257202 (2016).
[51] L. M. Sandratskii, Phys. Rev. B **90**, 184406 (2014).